# Spectroscopic and Electrical Properties of $[Cu(C_3Se_5)_2]^{2-}$ and $[Ni(C_3Se_5)_2]^{2-}$ Anion Complexes and *X*-Ray Crystal Structures of $[NMe_4]_2[Cu(C_3Se_5)_2]\cdot 2MeCN$ and $[NBu^n_4][Ni(C_3Se_5)_2]$†

**Gen-etsu Matsubayashi* and Akito Yokozawa**
*Department of Applied Chemistry, Faculty of Engineering, Osaka University, Yamadaoka, Suita, Osaka 565, Japan*

The complexes $[epy]_2[Cu(C_3Se_5)_2]\cdot MeCN$ (**1**) [epy = *N*-ethylpyridinium; $C_3Se_5^{2-}$ = 4,5-di(hydroseleno)-1,3-diselenole-2-selonate], $[NMe_4]_2[Cu(C_3Se_5)_2]\cdot 2MeCN$ (**2**), $[NMe_4][Cu(C_3Se_5)_2]$ (**3**) and $[ttf]_{0.4}[Cu(C_3Se_5)_2]$ (**4**) [$ttf^{\cdot+}$ = radical cation of tetrathiafulvalene, 2-(1',3'-dithiol-2'-ylidene)-1,3-dithiole] have been prepared. Complexes $[NBu^n_4]_2[Ni(C_3Se_5)_2]$ (**5**) and $[NMe_4]_2[Ni(C_3Se_5)_2]\cdot 0.5MeCN$ (**6**) have been oxidized electrochemically under a controlled current in acetonitrile or acetone to afford $[NBu^n_4][Ni(C_3Se_5)_2]$ (**7**), $[NBu^n_4]_{0.25}[Ni(C_3Se_5)_2]$ (**8**), and $[NMe_4]_{0.33}[Ni(C_3Se_5)_2]$ (**9**). All the complexes behave as semiconductors. Although complexes (**1**)—(**3**), (**5**), and (**6**) exhibit electrical conductivities of $1 \times 10^{-7}$—$1 \times 10^{-8}$ S cm$^{-1}$ for compacted pellets at 25 °C, conductivities of $1.4 \times 10^{-5}$ for (**4**) (compacted pellet), $2.0 \times 10^{-4}$ for (**7**) (crystal), 0.21 for (**8**), and 0.056 S cm$^{-1}$ for (**9**) (compacted pellets) were observed. A single-crystal *X*-ray structure analysis of (**2**) reveals that the $CuSe_4$ geometry around the copper(II) ion is substantially distorted from square planar, with a dihedral angle of 53.7° between the two diselenolate ligand planes. Additionally the anionic moieties form a two-dimensional molecular sheet through some interligand selenium–selenium contacts in the crystal phase. The orthorhombic crystal, space group *Ibam*, has cell dimensions $a$ = 10.289(3), $b$ = 23.367(6), $c$ = 15.519(7) Å, and $Z$ = 4. Block-diagonal least-squares refinement, based on 704 reflections [$|F_o| > 3\sigma(F)$], converged at $R$ = 0.065. An *X*-ray structure analysis of (**7**) reveals an almost square-planar geometry of the $[Ni(C_3Se_5)_2]^-$ anion, which forms a one-dimensional arrangement through several selenium–selenium contacts. The crystals are monoclinic, space group $P2_1/c$, with $a$ = 21.088(3), $b$ = 13.494(1), $c$ = 12.3818(9) Å, β = 106.17(1) °, and $Z$ = 4. The refinement, based on 3 127 reflections [$|F_o| > 3\sigma(F)$], converged at $R$ = 0.067. Electronic absorption, i.r., e.s.r., and *X*-ray photoelectron spectra of these complexes are described.

Recently metal complexes with the 4,5-dimercapto-1,3-dithiole-2-thionate ligand ($C_3S_5^{2-}$) have attracted much attention owing to their metallic behaviour through sulphur–sulphur molecular interactions,[1,2] of which $[ttf][Ni(C_3S_5)_2]_2$ [$ttf^{\cdot+}$ = radical cation of tetrathiafulvalene, 2-(1',3'-dithiol-2'-ylidene)-1,3-dithiole],[2] $[NMe_4][Ni(C_3S_5)_2]_2$,[3] and $[ttf][Pd(C_3S_5)_2]_2$[4] were reported to be superconductors. Since selenium has more spatially extended and diffuse orbitals than sulphur, metal complexes of the selenium analogue of the $C_3S_5^{2-}$ ligand, $C_3Se_5^{2-}$ [4,5-di(hydroseleno)-1,3-diselenole-2-selonate], may also become good electrical conductors through more effective selenium–selenium molecular interactions. However, very few studies of $C_3Se_5^{2-}$–metal complexes have been reported.[5–8] This paper reports the crystal structures of $[NMe_4]_2[Cu(C_3Se_5)_2]\cdot 2MeCN$ and $[NBu^n_4][Ni(C_3Se_5)_2]$ and their electronic absorption, i.r., e.s.r., and *X*-ray photoelectron spectra as well as electrical conductivites. A preliminary report of the crystal structure of the former complex has appeared.[9]

## Experimental

*Preparation.*—$[epy]_2[Cu(C_3Se_5)_2]\cdot MeCN$ (**1**) [epy = *N-Ethylpyridinium*) *and* $[NMe_4][Cu(C_3Se_5)_2]$ (**3**).—4,5-Bis(benzoylseleno)-1,3-diselenole-2-selone[10] (150 mg, 230 μmol), prepared from $[PPh_4]_2[Zn(C_3Se_5)_2]$,[8] was dissolved in a methanol solution (10 cm$^3$) containing sodium metal (12 mg, 520 μmol) and the solution was stirred for 30 min at room temperature. To the resulting solution of $Na_2[C_3Se_5]$ was added a methanol solution (2 cm$^3$) of an excess of $[epy][ClO_4]$, followed by a methanol solution (2 cm$^3$) of $CuCl_2$ (16 mg, 120 μmol). Black solids precipitated immediately, which were collected by centrifugation, washed with methanol and water, and dried *in vacuo*. They were recrystallized from acetonitrile to afford black microcrystals of $[epy]_2[Cu(C_3Se_5)_2]\cdot MeCN$ (**1**) (yield, 65%) (Found: C, 22.45; H, 2.2; N, 3.35. Calc. for $C_{22}H_{23}CuN_3Se_{10}$: C, 22.35; H, 1.95; N, 3.35%).

A similar reaction, but using $[NMe_4]Br$ instead of $[epy][ClO_4]$, afforded black microcrystals of $[NMe_4][Cu(C_3Se_5)_2]$ (**3**) (yield, 97%) (Found: C, 12.65; H, 1.35; N, 1.4. Calc. for $C_{10}H_{12}CuNSe_{10}$: C, 12.0; H, 1.2; N, 1.4%). The solids were recrystallized from acetonitrile to afford black plates of $[NMe_4]_2[Cu(C_3Se_5)_2]\cdot 2MeCN$ (**2**). The formula of (**2**) was confirmed by an *X*-ray structure analysis.

*Preparation of* $[ttf]_{0.4}[Cu(C_3Se_5)_2]$ (**4**).—An acetonitrile solution (10 cm$^3$) of (**3**) (21 mg, 21 μmol) was added with stirring to an acetonitrile solution (15 cm$^3$) of $[ttf]_3[BF_4]_2$[11] (31 mg, 40

† Bis(tetramethylammonium) bis[4,5-di(hydroseleno)-1,3-diselenole-2-selonato-*Se*$^4$*Se*$^5$]cuprate(II)–acetonitrile(1/2) and tetrabutylammonium bis[4,5-di(hydroseleno)-1,3-diselenole-2-selonato-*Se*$^4$*Se*$^5$]-nickelate(III).

*Supplementary data available:* see Instructions for Authors, *J. Chem. Soc., Dalton Trans.*, 1990, Issue 1, pp. xix–xxii.

*Non-S.I. unit employed:* eV ≈ $1.6 \times 10^{-19}$ J.

**Table 1.** Experimental data and structure refinement details[a] for complexes (2) and (7)

| Complex | (2) | (7) |
|---|---|---|
| Formula | $C_{18}H_{30}CuN_4Se_{10}$ | $C_{22}H_{36}NNiSe_{10}$ |
| $M$ | 1 150.6 | 1 162.8 |
| Crystal size/mm | 0.10 × 0.16 × 0.42 | 0.05 × 0.05 × 0.55 |
| Crystal system | Orthorhombic | Monoclinic |
| Space group | *Ibam* | $P2_1/c$ |
| $a$/Å | 10.289(3) | 21.088(3) |
| $b$/Å | 23.367(6) | 13.494(1) |
| $c$/Å | 15.519(7) | 12.381 8(9) |
| α/° | 90 | 90 |
| β/° | 90 | 106.17(1) |
| γ/° | 90 | 90 |
| $U$/Å$^3$ | 3 731(2) | 3 383.8(6) |
| $Z$ | 4 | 4 |
| $D_c$/g cm$^{-3}$ | 2.057(1) | 2.283(1) |
| $F$(000) | 2 120.0 | 2 172.0 |
| Radiation/Å | Mo-$K_\alpha$ (λ = 0.710 69) | Cu-$K_\alpha$ (λ = 1.5418) |
| μ/cm$^{-1}$ | 110.8 | 149.6 |
| Scan interval/° min$^{-1}$ | 8 | 8 |
| Collected octants | $h, k, -l$ | $\pm h, k, l$ |
| No. of data collected at room temperature | 1 865 | 5 336 |
| No. of independent data with $\|F_o\| > 3\sigma(F)$ | 704 | 3 127 |
| Absorption correction range[b] | 1.00—0.33 | 1.00—0.38 |
| $R$ | 0.065 | 0.067 |
| $R'$[c] | 0.105 | 0.084 |

[a] Rigaku-AFC diffractometers; scan ranges $3 < 2\theta < 50°$ for (2) and $4 < 2\theta < 120°$ for (7). [b] A. C. T. North, D. C. Phillips, and F. C. Matheus, *Acta Crystallogr., Sect. A*, 1968, **4**, 351. [c] $[\Sigma w(\|F_o\| - \|F_c\|)^2/\Sigma w\|F_o\|^2]^{\frac{1}{2}}$, where $w^{-1} = \sigma^2(F_o) + 0.0015F_o^2$ for (2) and $w^{-1} = \sigma^2(F_o) + 0.001F_o^2$ for (7).

**Table 2.** Fractional atomic co-ordinates for $[NMe_4]_2[Cu(C_3Se_5)_2]$·2MeCN (2) with estimated standard deviations (e.s.d.s) in parentheses

| Atom | $x$ | $y$ | $z$ |
|---|---|---|---|
| Cu | 0 | 0 | 0.25 |
| Se(1) | 0.152 4(4) | 0.068 1(1) | 0.199 6(3) |
| Se(2) | 0.133 2(3) | 0.205 8(1) | 0.204 4(3) |
| Se(3) | 0 | 0.327 0(2) | 0.25 |
| N(1) | 0.193(5) | 0.108(2) | 0.5 |
| N(2) | 0.160(7) | 0.379(3) | 0.5 |
| C(1) | 0.052(3) | 0.133(1) | 0.233(2) |
| C(2) | 0 | 0.246(2) | 0.25 |
| C(3) | 0.258(6) | 0.123(2) | 0.421(3) |
| C(4) | 0.204(9) | 0.052(3) | 0.5 |
| C(5) | 0.053(7) | 0.123(3) | 0.5 |
| C(6) | 0.126(9) | 0.318(3) | 0.5 |
| C(7) | 0.07(1) | 0.261(4) | 0.5 |

μmol). Black solids of $[ttf]_{0.4}[Cu(C_3Se_5)_2]$ immediately precipitated, which were collected by centrifugation, washed with acetonitrile, and dried *in vacuo* (yield, 77%) (Found: C, 9.7; H, 0.5. Calc. for $C_{7.6}H_{1.6}CuS_{1.6}Se_{10}$: C, 10.0; H, 0.2%). The presence of the $ttf^{\bullet+}$ radical cation was confirmed by e.s.r. spectroscopy.

*Preparation of* $[NBu^n_4]_2[Ni(C_3Se_5)_2]$ (5) *and* $[NMe_4]_2[Ni(C_3Se_5)_2]$·0.5MeCN (6)—4,5-Bis(benzoylseleno)-1,3-diselenole-2-selone (150 mg, 230 μmol) was dissolved in a methanol solution (10 cm$^3$) containing sodium metal (12 mg, 520 μmol). To this was added $[NMe_4]Br$ (38 mg, 250 μmol), followed by a methanol solution (3 cm$^3$) of bis(acetylacetonato)nickel, (30 mg, 120 μmol). Brown solids precipitated immediately, which were collected by filtration and dried *in vacuo*. They were recrystallized from acetonitrile to afford brown microcrystals of $[NMe_4]_2[Ni(C_3Se_5)_2]$·0.5MeCN (6) (50% yield) (Found: C, 16.95; H, 2.25; N, 3.45. Calc. for $C_{15}H_{25.5}N_{2.5}NiSe_{10}$: C, 16.55; H, 2.35; N, 3.2%). Similarly, $[NBu^n_4]_2[Ni(C_3Se_5)_2]$ (5) was prepared by using $[NBu^n_4][ClO_4]$ instead of $[NMe_4]Br$ and recrystallized from acetonitrile (72% yield) (Found: C, 32.3; H, 5.2; N, 1.85. Calc. for $C_{38}H_{72}N_2NiSe_{10}$: C, 32.45; H, 5.15; N, 2.0%).

*Preparation of Oxidized* $[Ni(C_3Se_5)_2]^{n-}$ $(n \leqslant 1)$ *Complexes.*—An acetonitrile solution (50 cm$^3$) containing complex (5) (22 mg, 16 μmol) and $[NBu^n_4][ClO_4]$ (1.28 g, 3.7 mmol) was subjected to a controlled-current (1 μA) electrolysis for 16 d under a nitrogen atmosphere in an H-cell consisting of platinum wire (for both the anode and cathode). Dark red needles of $[NBu^n_4][Ni(C_3Se_5)_2]$ (7) were collected from the anode and dried *in vacuo* (20% yield). The composition of the crystals was determined by an *X*-ray structure analysis. A similar controlled-current electrolysis of (5) dissolved in acetone afforded black microcrystals of $[NBu^n_4]_{0.25}[Ni(C_3Se_5)_2]$ (8) on the anode, which were collected and dried *in vacuo* (15% yield) (Found: C, 12.0; H, 1.0; N, 0.6. Calc. for $C_{10.0}H_{9.0}N_{0.25}NiSe_{10}$: C, 12.2; H, 0.9; N, 0.4%).

A controlled-current electrolysis of (6) in acetonitrile, containing an excess of $[NMe_4][ClO_4]$ as electrolyte, by a similar procedure to that described for the tetrabutylammonium complexes yielded black microcrystals of $[NMe_4]_{0.33}[Ni(C_3Se_5)_2]$ (9) (23% yield) (Found: C, 9.15; H, 0.45; N, 0.6. Calc. for $C_{7.3}H_{4.0}N_{0.33}NiSe_{10}$: C, 9.3; H, 0.4; N, 0.5%).

Complex (7) was also prepared by aerial oxidation of (5) (280 mg, 200 μmol) dissolved in 1,2-dichloroethane (100 cm$^3$). The solution was stirred for 24 h at room temperature, concentrated to one third of its volume, and hexane (50 cm$^3$) added to afford dark red solids. These were collected by filtration and dried *in vacuo* (65% yield) (Found: C, 23.1; H, 3.35; N, 1.3. Calc. for $C_{22}H_{36}NNiSe_{10}$: C, 22.7; H, 3.1; N, 1.2%).

*X-Ray Crystal Structure Determinations of* $[NMe_4]_2[Cu(C_3Se_5)_2]$·2MeCN (2) *and* $[NBu^n_4][Ni(C_3Se_5)_2]$ (7).—Crystal data and details of the measurements are listed in Table 1. The unit-cell parameters were determined from 25 independent reflections having $23 < 2\theta < 26°$ (Mo-$K_\alpha$ radiation) and $35 < 2\theta < 54°$ (Cu-$K_\alpha$ radiation) for (2) and (7), respectively. For (2), systematic absences (*hkl*, with $h + k + l$ odd; *h0l*, with *l* odd; *hk*0, with $h + k$ odd; and 0*kl*, with *k* odd) indicated two possible space groups, *Iba*2 or *Ibam*; the latter was confirmed from the successful analysis. For (7), systematic absences (*h*0*l*, with *l* odd; 0*k*0, with *k* odd; and 00*l*, with *l* odd) enabled assignment of space group $P2_1/c$.

The structures of both complexes were solved according to the direct (MULTAN) method.[12] Subsequent Fourier maps revealed the positions of all the non-hydrogen atoms which were refined anisotropically by the block-diagonal least-squares procedure. Atomic scattering factors used in the refinement were taken from ref. 13. Atomic positional parameters for complexes (2) and (7) are shown in Tables 2 and 3, respectively.

Crystallographic calculations were performed using the programs of Professor K. Nakatsu, Kwansei Gakuin University, on an ACOS 900S computer at the Research Centre for Protein Engineering, Institute for Protein Research, Osaka University. Figures 1—5 were drawn by the local version of the ORTEP II program.[14]

Additional material available from the Cambridge Crystallographic Data Centre comprises thermal parameters and remaining bond lengths and angles.

*Physical Measurements.*—Electronic absorption, i.r.,[15] e.s.r.,

**Table 3.** Fractional atomic co-ordinates for $[NBu^n_4][Ni(C_3Se_5)_2]$ (**7**) with e.s.d.s in parentheses

| Atom | *x* | *y* | *z* | Atom | *x* | *y* | *z* |
|---|---|---|---|---|---|---|---|
| Ni | 0.258 5(1) | 0.241 8(2) | 0.519 5(2) | C(6) | 0.100 3(6) | 0.229 2(11) | 0.461 7(12) |
| Se(1) | 0.309 73(8) | 0.335 0(2) | 0.416 4(2) | C(7) | 0.750 8(7) | 0.400 4(10) | 0.162 2(11) |
| Se(2) | 0.464 81(9) | 0.381 1(2) | 0.444 2(2) | C(8) | 0.742 3(11) | 0.468 1(13) | 0.058 7(15) |
| Se(3) | 0.619 56(9) | 0.364 9(2) | 0.576 1(2) | C(9) | 0.720 0(9) | 0.403 7(14) | −0.045 4(17) |
| Se(4) | 0.508 78(8) | 0.243 3(2) | 0.653 3(2) | C(10) | 0.650 0(11) | 0.372 1(19) | −0.078 1(20) |
| Se(5) | 0.355 71(8) | 0.188 7(2) | 0.639 1(2) | C(11) | 0.695 8(7) | 0.525 4(12) | 0.265 7(14) |
| Se(6) | 0.207 76(8) | 0.156 3(2) | 0.629 7(2) | C(12) | 0.634 4(7) | 0.460 2(13) | 0.249 6(16) |
| Se(7) | 0.053 06(8) | 0.117 9(2) | 0.610 5(2) | C(13) | 0.573 3(9) | 0.526 6(15) | 0.241 1(17) |
| Se(8) | −0.102 13(9) | 0.150 8(2) | 0.498 6(2) | C(14) | 0.556 0(10) | 0.583 4(17) | 0.133 7(19) |
| Se(9) | 0.007 88(8) | 0.245 9(2) | 0.393 9(2) | C(15) | 0.770 7(7) | 0.388 8(11) | 0.368 6(11) |
| Se(10) | 0.161 18(8) | 0.289 8(1) | 0.397 1(2) | C(16) | 0.783 3(8) | 0.437 2(12) | 0.483 7(13) |
| N | 0.758 6(6) | 0.462 9(9) | 0.270 2(10) | C(17) | 0.795 7(9) | 0.360 8(12) | 0.576 1(14) |
| C(1) | 0.397 7(7) | 0.313 7(11) | 0.492 2(12) | C(18) | 0.807 8(10) | 0.408 2(16) | 0.693 9(15) |
| C(2) | 0.534 5(8) | 0.329 2(14) | 0.557 3(15) | C(19) | 0.812 4(7) | 0.541 7(11) | 0.284 5(13) |
| C(3) | 0.417 2(7) | 0.254 2(12) | 0.580 5(13) | C(20) | 0.882 9(7) | 0.495 1(13) | 0.299 6(14) |
| C(4) | 0.119 4(6) | 0.175 9(12) | 0.554 9(13) | C(21) | 0.931 7(8) | 0.582 3(13) | 0.333 2(17) |
| C(5) | −0.017 8(6) | 0.171 7(12) | 0.500 4(13) | C(22) | 1.005 7(9) | 0.546 4(15) | 0.344 5(19) |

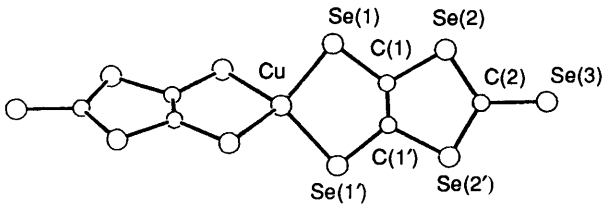


**Figure 1.** Molecular geometry of the $[Cu(C_3Se_5)_2]^{2-}$ anion of (**2**), together with the atom-labelling scheme

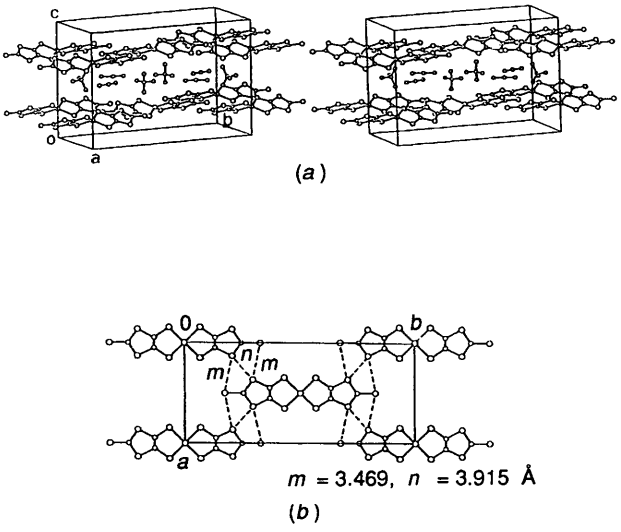


**Figure 2.** Stereoscopic packing diagram for $[NMe_4]_2[Cu(C_3Se_5)_2]\cdot 2MeCN$ (*a*) and selenium–selenium contacts among the $[Cu(C_3Se_5)_2]^{2-}$ anion moieties projected along the *c* axis (*b*)

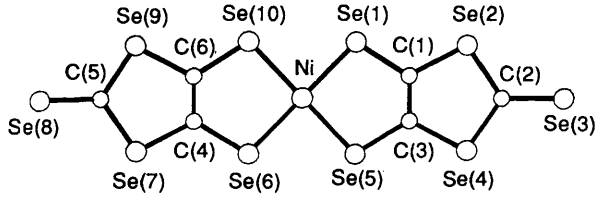


**Figure 3.** Molecular geometry of the anion moiety of $[NBu^n_4][Ni(C_3Se_5)_2]$ (**7**), together with the atom-labelling scheme

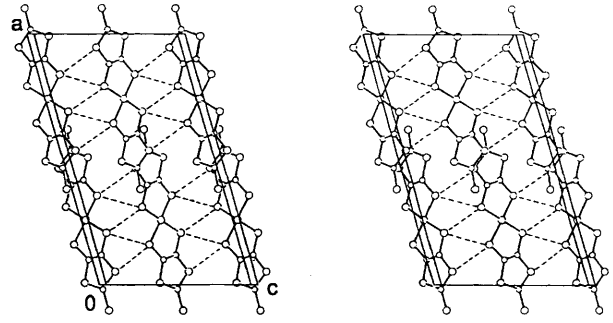


**Figure 4.** Stereoview of the packing of the anionic moieties of $[NBu^n_4][Ni(C_3Se_5)_2]$ (**7**) along the *b* axis; dashed lines represent non-bonded Se · · · Se contacts less than 4.0 Å

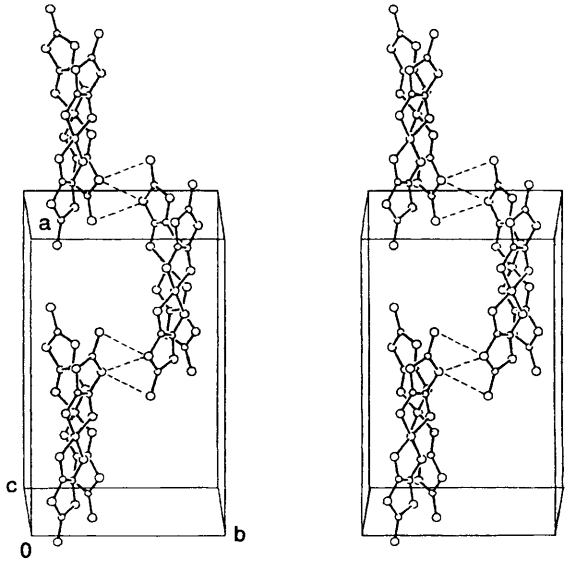


**Figure 5.** Stereoview of the packing of the anionic moieties of $[NBu^n_4][Ni(C_3Se_5)_2]$ (**7**) along the *c* axis; dashed lines represent non-bonded Se · · · Se contacts less than 4.0 Å

and *X*-ray photoelectron spectra [16] were measured as described elsewhere. Electrical resistivities of the complexes were measured for compacted pellets [(**1**)—(**6**), (**8**), and (**9**)] and for a crystal [(**7**)] by the conventional two-probe method.[15] Cyclic

**Table 4.** Selected bond distances (Å) and angles (°) with e.s.d.s in parentheses for $[NMe_4]_2[Cu(C_3Se_5)_2]\cdot 2MeCN$ (**2**)

| | | | |
|---|---|---|---|
| Cu–Se(1) | 2.366(3) | Se(1)–C(1) | 1.90(3) |
| Se(2)–C(1) | 1.95(3) | Se(2)–C(2) | 1.81(2) |
| Se(3)–C(2) | 1.89(4) | C(1)–C(1′) | 1.21(4) |
| Se(1)–Cu–Se(1′) | 95.6(1) | Cu–Se(1)–C(1) | 94.9(9) |
| Se(1)–C(1)–Se(2) | 114(2) | Se(1)–C(1)–C(1′) | 127(2) |
| Se(2)–C(1)–C(1′) | 119(2) | C(1)–Se(2)–C(2) | 93(1) |
| Se(2)–C(2)–Se(3) | 121(1) | Se(2)–C(2)–Se(2′) | 117(2) |

**Table 5.** Selected bond distances (Å) and angles (°) with e.s.d.s in parentheses for $[NBu^n_4][Ni(C_3Se_5)_2]$ (**7**)

| | | | |
|---|---|---|---|
| Ni–Se(1) | 2.269(3) | Se(5)–C(3) | 1.874(16) |
| Ni–Se(5) | 2.284(3) | Se(6)–C(4) | 1.855(12) |
| Ni–Se(6) | 2.270(3) | Se(7)–C(4) | 1.892(16) |
| Ni–Se(10) | 2.279(3) | Se(7)–C(5) | 1.867(13) |
| Se(1)–C(1) | 1.853(13) | Se(8)–C(5) | 1.794(14) |
| Se(2)–C(1) | 1.912(16) | Se(9)–C(5) | 1.853(17) |
| Se(2)–C(2) | 1.862(16) | Se(9)–C(6) | 1.909(12) |
| Se(3)–C(2) | 1.808(17) | Se(10)–C(6) | 1.877(15) |
| Se(4)–C(2) | 1.848(20) | C(1)–C(3) | 1.326(21) |
| Se(4)–C(3) | 1.896(13) | C(4)–C(6) | 1.323(21) |
| Se(1)–Ni–Se(5) | 93.2(1) | Ni–Se(10)–C(6) | 100.9(4) |
| Se(1)–Ni–Se(10) | 87.1(1) | Se(1)–C(1)–C(3) | 123.3(12) |
| Se(5)–Ni–Se(6) | 86.5(1) | Se(2)–C(1)–C(3) | 117.2(10) |
| Se(6)–Ni–Se(10) | 93.2(1) | Se(2)–C(2)–Se(4) | 114.1(9) |
| C(1)–Se(2)–C(2) | 94.9(7) | Se(5)–C(3)–C(1) | 121.0(10) |
| C(2)–Se(4)–C(3) | 95.1(7) | Se(6)–C(4)–C(6) | 122.1(12) |
| Ni–Se(5)–C(3) | 101.2(4) | Se(7)–C(4)–C(6) | 117.8(10) |
| Ni–Se(6)–C(4) | 101.7(5) | Se(7)–C(5)–Se(9) | 113.3(7) |
| C(4)–Se(7)–C(5) | 95.5(6) | Se(9)–C(6)–C(4) | 118.2(11) |
| C(5)–Se(9)–C(6) | 95.1(6) | Se(10)–C(6)–C(4) | 122.0(10) |

voltammograms were measured in acetonitrile as described previously.[17]

## Results and Discussion

*Crystal Structure of* $[NMe_4]_2[Cu(C_3Se_5)_2]\cdot 2MeCN$ (**2**).—Figure 1 illustrates the geometry of the $[Cu(C_3Se_5)_2]^{2-}$ anion of complex (**2**), together with the atom-labelling scheme. Selected bond distances and angles are summarized in Table 4. The copper atom, as well as C(2) and Se(3), is located on the $C_2$ axis, and is ligated with four equivalent selenium atoms. The $C_3Se_5$ moiety is almost planar (±0.010 Å), similar to $[PPh_4]_2[Zn(C_3Se_5)_2]$ reported previously.[8] Since the C(2)–Se(2) and C(2)–Se(3) bonds are appreciably shorter than C(1)–Se(1) and C(1)–Se(2), electron delocalization seems to be more effective in the terminal $CSe_3$ group than in the $C_2Se_4$ moiety; in accordance with this the C(1)–C(1′) bond is short. This behaviour resembles that for $[PPh_4]_2[Zn(C_3Se_5)_2]$ in which electron delocalization within the $CSe_3$ moiety was supported from both *X*-ray crystallography and $^{77}Se$ n.m.r. spectroscopy.[8] On the other hand, in $[epy]_2[Cu(C_3S_5)_2]$[17] the terminal C–S bond (1.654 Å) is considerably shorter compared with the other C–S bonds (av. 1.733 Å), and $[NBu^n_4][Ni(C_3S_5)_2]$ also showed the same tendency (terminal C–S bond, av. 1.63 Å; other C–S bonds, 1.74 Å).[18] The electron delocalization occurs through the central $C_2S_4$ part of the $C_3S_5^{2-}$ ligand, which is in a direct contrast to the $C_3Se_5^{2-}$ ligand.

Although no comparative Cu–Se bond lengths for [diselenolato(2−)]copper(II) complexes are available, the Cu–Se bond lengths of complex (**2**) are somewhat shorter than those of bis[*N*,*N*-diethyldiselenocarbamato]copper(II) (av. 2.430 Å),[19] which arises from the difference in charges of the ligands. Moreover, the Cu–Se bond of complex (**2**) is longer than the Cu–S bond [av. 2.272(3) Å] of the $[Cu(C_3S_5)_2]^{2-}$ anion.[17] This difference arises mainly from a larger atomic covalent radius for selenium (1.17 Å) than for sulphur (1.04 Å).[20] However, the difference (0.09 Å) between the Cu–Se and Cu–S distances is appreciably smaller than that (0.17 Å) between Se(1)–C(1) [1.90(3) Å] and the corresponding S–C bond [av. 1.779(9) Å] of the $[Cu(C_3S_5)_2]^{2-}$ anion, indicating that the Cu–Se bond is of higher order than Cu–S.

The $[Cu(C_3Se_5)_2]^{2-}$ anion shown in Figure 1 exhibits a non-planar geometry with a dihedral angle of 53.7° between the least-squares planes of the two ligands. This is very uncommon since bis(dithiolato)- and bis(diselenolato)-metal complexes usually assume planar geometries,[21,22] although very few bis[diselenolato(2−)]metal complexes have been determined crystallographically.[23,24] The present finding is very similar to the unusual non-planar geometry observed in $[epy]_2[Cu(C_3S_5)_2]$,[17] where a dihedral angle of 57.3° between the two dithiolato ligand planes is observed. The complex $[mb]_2[Cu(C_4N_2S_2)_2]\cdot(CH_3)_2CO$ [mb = methylene blue cation, 3,7-bis(dimethylamino)phenothiazin-5-ium; $C_4N_2S_2^{2-}$ = 1,2-dicyanoethylene-1,2-dithiolate] also has a dihedral angle of 47.3° between the two ligands.[25] Thus, two dithiolato(2−) or diselenolato(2−) ligands may form a non-planar geometry around copper(II) to reduce repulsion between the negatively charged sulphur or selenium atoms of the ligands.

Figure 2 shows the crystal structure of complex (**2**) and selenium–selenium contacts among the anion moieties. The copper atoms which are located on the special positions (0, 0, ¼) and (½, ½, ¼) interact with each other through interligand selenium–selenium contacts (3.47—3.92 Å) within the sum of van der Waals radius of selenium (4.0 Å),[20] so forming a two-dimensional sheet of interacting anions parallel to the *ab* plane. The spacing between the sheets is 7.760 Å. The tetramethylammonium cations and acetonitrile molecules are alternatively arranged along the *b* axis strictly midway between the sheets. The sheet formation can be compared with the one-dimensional molecular interaction through sulphur–sulphur contacts observed for $[epy]_2[Cu(C_3S_5)_2]$.[17] Noting the extension from a one- to two-dimensional molecular interaction, selenium with diffuse extended *p* and *d* orbitals seems indeed to be more effective than sulphur in such interactions.

*Crystal Structure of* $[NBu^n_4][Ni(C_3Se_5)_2]$ (**7**).—The molecular structure of the anion moiety is illustrated in Figure 3 with the atom-labelling scheme. Selected bond lengths and angles are listed in Table 5. The nickel atom is co-ordinated by four selenium atoms. The $C_3Se_5$ moieties are also almost planar (±0.010 Å). The terminal C–Se bonds (av. 1.801 Å) are considerably shorter compared with the other C–Se bonds (av. 1.875 Å). Electron delocalization occurs through the central $C_2Se_4$ skeleton of the $C_3Se_5^{2-}$ ligands, as for $[NBu^n_4][Ni(C_3S_5)_2]$.[18] The geometry around the nickel atom is slightly distorted from planarity with a dihedral angle of 6.0° between the two ligand planes. This closely resembles $[NBu^n_4][Ni(C_3S_5)_2]$ for which the dihedral angle between the two ligand planes is 6.1°.[18] These structures however do show some deviation from the essentially planar geometry observed around the metal atom in other four-co-ordinate $NiS_4$ and $NiSe_4$ complexes.[21,22,26,27]

Comparing the structure of (**7**) with that of $[NBu^n_4][Ni(C_3S_5)_2]$, the difference (0.12 Å) between the Ni–Se and Ni–S distances is similar to that (0.14 Å) between the average value (1.855 Å) of Se(1)–C(1), Se(5)–C(3), Se(6)–C(4), and Se(10)–C(6) distances and the corresponding S–C average bond length (1.725 Å) of the $[Ni(C_3S_5)_2]^-$ anion. Thus, no

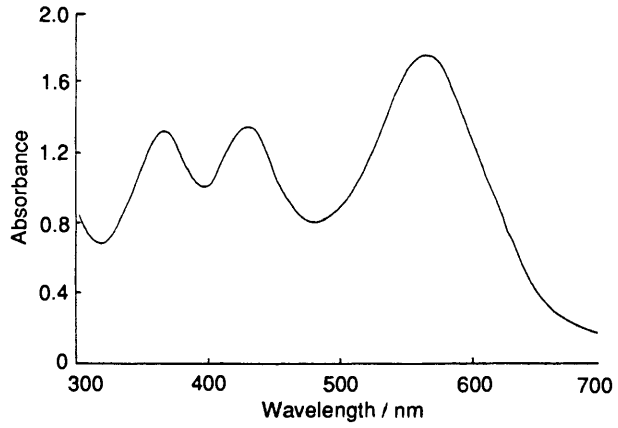


**Figure 6.** Electronic absorption spectra of $[epy]_2[Cu(C_3Se_5)_2]$·MeCN (**1**) ($1.5 \times 10^{-4}$ mol $dm^{-3}$) in acetonitrile

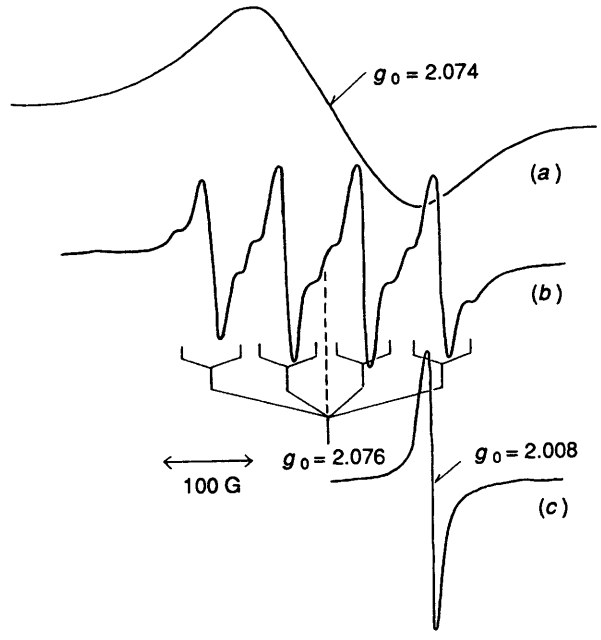


**Figure 7.** E.s.r. spectra of $[epy]_2[Cu(C_3Se_5)_2]$·MeCN (**1**) in the solid state (*a*) and in acetonitrile at room temperature (*b*), together with that of $[ttf]_{0.4}[Cu(C_3Se_5)_2]$ (**4**) in the solid state (*c*)

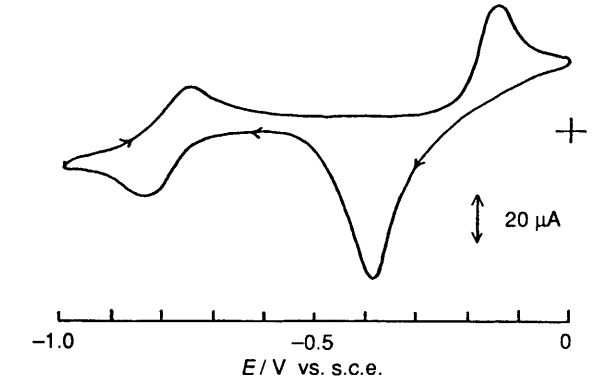


**Figure 8.** Cyclic voltammogram of the $[Cu(C_3Se_5)_2]^{2-}$ species ($5.5 \times 10^{-4}$ mol $dm^{-3}$) in acetonitrile: 0.1 mol $dm^{-3}$ $[NBu^n_4][ClO_4]$, scan rate, 0.1 V $s^{-1}$

appreciable high-bond order is deduced in the Ni–Se bonds compared with the Se–C bonds, in contrast to the $[Cu(C_3Se_5)_2]^{2-}$ anion.

The Ni–Se distances [av. 2.275(4) Å] are similar to those of $[NBu^n_4]_2[Ni(bds)_2]$ [bds = *o*-benzenediselenolate-(2−)] (2.259 Å)[26] and $[tmtsf]_2[Ni(tds)_2]$ {$tmtsf^{\bullet+}$ = the radical cation of tetramethyltetraselenafulvalene, 2-(4′,5′-dimethyl-1′,3′-diselenol-2′-ylidene)-4,5-dimethyl-1,3-diselenole; tds = [2,2-bis(trifluoromethyl)ethylene]-1,1-diselenolate(2−)} (av. 2.255 Å),[27] the only other structurally characterized bis(diselenolene)nickel complexes.

Figure 4 shows the molecular packing diagram of the anion moieties of the complex projected along the *b* axis. Among the anions, several selenium–selenium contacts (3.603—3.951 Å) within the sum of the van der Waals radius of selenium are observed. The almost planar $[Ni(C_3Se_5)_2]^-$ moieties are located in a zigzag arrangement with a dihedral angle of 74.1° between them to form a one-dimensional anionic chain along the *c* axis. These chains interact with each other through selenium atoms [Se(2)···Se(2′), 3.643(3); Se(2)···Se(3′), 3.838(3); Se(3)···Se(2′), 3.837(3) Å] to form another molecular interaction along the *c* axis (see Figure 5). Another closest selenium–selenium contact between the anionic moieties is 4.101(3) Å.

*Spectroscopic and Oxidation Properties of the* $[Cu(C_3Se_5)_2]^{2-}$ *and* $[Ni(C_3Se_5)_2]^{2-}$ *Complexes.*—The electronic absorption spectrum of (**1**) dissolved in acetonitrile is illustrated in Figure 6. The intense bands at 367 and 563 nm are ascribed to the ligand π—π* transitions, which occur at longer wavelengths than the corresponding bands (310 and 540 nm) of the sulphur analogue, $[Cu(C_3S_5)_2]^{2-}$.[17] This finding is also the same as that observed for the corresponding zinc(II) complexes.[8] Since the band at 400 nm observed for the $[Cu(C_3S_5)_2]^{2-}$ anion is reasonably assigned to a Cu ⟵ S charge transfer (c.t.) transition based on the c.t. bands of some copper(II)–thiolate complexes,[28–30] the band at 429 nm of the $[Cu(C_3Se_5)_2]^{2-}$ species is reasonably ascribed to a Cu ⟵ Se c.t. transition. This band also occurs at a longer wavelength than the Cu ⟵ S c.t. band, in accordance with the higher bond order of Cu–Se over Cu–S as described above.

Figure 7 shows the e.s.r. spectra of (**1**) both in the solid state and in acetonitrile solution at room temperature, together with the powder spectrum of (**4**) in the solid state. Complex (**1**) exhibits an apparently isotropic spectrum ($g$ = 2.074) in the solid state, which can be compared with the anisotropic spectrum found for $[epy]_2[Cu(C_3S_5)_2]$ ($g_{\|}$ = 2.092 and $g_{\perp}$ = 2.026).[17] In the solution spectrum the isotropic $^{63/65}Cu$ hyperfine structure [$|A_0(^{63/65}Cu)|$ = 73.0 × $10^{-4}$ $cm^{-1}$] together with $^{77}Se$ coupling [$|A_0(^{77}Se)|$ = 51.7 × $10^{-4}$ $cm^{-1}$] is observed. A drastic decrease in $A_0(^{63/65}Cu)$ values was proposed for $CuS_4$ complexes upon some distortion from a square-planar to a tetrahedral geometry around the copper atom.[31] The $[Cu(C_3S_5)_2]^{2-}$ anion exhibits a low $A_0(^{63/65}Cu)$ (66.5 × $10^{-4}$ $cm^{-1}$) in acetonitrile, indicating a distorted $CuS_4$ geometry in solution. However, the value of $A_0(^{63/65}Cu)$ for $[Cu(C_3Se_5)_2]^{2-}$ in acetonitrile is close to that of a square-planar $CuSe_4$ species, bis[*N*,*N*-diethyldiselenocarbamato]copper(II) (74.7 × $10^{-4}$ $cm^{-1}$).[32] This finding suggests that the $[Cu(C_3Se_5)_2]^{2-}$ anion assumes a planar geometry around the copper(II) ion in solution.

Complex (**3**) shows no e.s.r. signal in the solid state, suggesting that metal-centred oxidation occurs to give a copper(III) centre and non-oxidized ligand moieties. In accordance with this, the ν(C=C) i.r. band of the ligand occurs at 1 400 $cm^{-1}$ which is close to that of the $[Cu(C_3Se_5)_2]^{2-}$ species (1 410 $cm^{-1}$).

Complex (**4**) shows a sharp e.s.r. signal ($g$ = 2.008) (Figure 7),

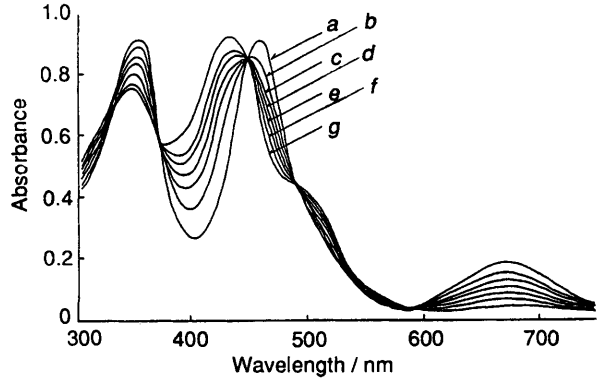


**Figure 9.** Electronic absorption spectra of $[NBu^n_4]_2[Ni(C_3Se_5)_2]$ (**5**) ($8.2 \times 10^{-5}$ mol $dm^{-3}$) in 1,2-dichloroethane in air. Time (h): (*a*), 0; (*b*), 1; (*c*), 2; (*d*), 3; (*e*), 4; (*f*), 5; (*g*), 20

which is ascribed to the $ttf^{\bullet+}$ radical cation.[33] However, no signal due to the $Cu(C_3Se_5)_2$ anion is observed.

A cyclic voltammogram of the $[Cu(C_3Se_5)_2]^{2-}$ anion in acetonitrile is shown in Figure 8. Oxidation peak potentials at −0.8 and −0.15 V [*vs.* saturated calomel electrode (s.c.e.)] correspond to the oxidation processes of $[Cu(C_3Se_5)_2]^{3-}$ and $[Cu(C_3Se_5)_2]^{2-}$ species, respectively. Although the $[Cu(C_3Se_5)_2]^{2-}$–$[Cu(C_3S_5)_2]^{-}$ redox process is irreversible, the oxidation peak potential is 0.17 V lower than that of the $[Cu(C_3S_5)_2]^{2-}$–$[Cu(C_3S_5)_2]^{-}$ process.[17] This behaviour is similar to the observation that oxidation potentials of $[M(C_3Se_5)_2]^{n-}$–$[M(C_3Se_5)_2]^{(n-1)-}$ are 0.06—0.39 V lower than those of $[M(C_3S_5)_2]^{n-}$–$[M(C_3S_5)_2]^{(n-1)-}$ ($M = Ni^{II}$ or $Pd^{II}$, $n = 2$; $Au^{III}$, $n = 1$).[34]

Although complex (**3**) appears to be a copper(III) complex, exhibiting no e.s.r. signal in the solid state, an acetonitrile solution of this complex gave appreciable signals in the e.s.r. spectrum, essentially the same as those of (**1**), indicating the formation of the copper(II) species in solution (see Figure 8). Interestingly recrystallisation of complex (**3**) from acetonitrile afforded crystals of (**2**) which were scarcely soluble in organic solvents. Although oxidation of the $[Cu(C_3Se_5)_2]^{2-}$ species by iodine in solution resulted in decomposition of the $Cu(C_3Se_5)_2$ skeleton, oxidation of the $[Cu(C_3Se_5)_2]^{2-}$ species with $ttf^{\bullet+}$ (the redox potential of $ttf^0/ttf^{\bullet+}$, 0.33 V *vs.* s.c.e.[35]) afforded a further oxidized species, (**4**), as a black solid.

As illustrated in Figure 9, the absorption spectrum of the nickel(II) complex, (**5**), changes with time in 1,2-dichloroethane solution in air owing to aerial oxidation of $[Ni(C_3Se_5)_2]^{2-}$ to $[Ni(C_3Se_5)_2]^{-}$ with the final spectrum being identical with that of $[NBu^n_4][Ni(C_3Se_5)_2]$ (**7**) obtained by electrochemical oxidation of the $[Ni(C_3Se_5)_2]^{2-}$ species in acetonitrile. The stable oxidation process of this anion is reflected in the reversible redox potential at 0.11 V *vs.* s.c.e. which was observed in a cyclic voltammogram of complex (**5**) in acetonitrile.[5]

Although complex (**7**) is formally in the $Ni^{III}$ state, the binding energy (854.4 eV) of the Ni $2p_{\frac{3}{2}}$ electrons of this complex as determined by *X*-ray photoelectron spectroscopy is very close to that (854.2 eV) of complex (**5**). This suggests a ligand-centred oxidation, as observed for $[NBu^n_4][M(C_3S_5)_2]$ (M = Ni, Pd, or Pt).[36] Furthermore, the ν(C=C) band in the i.r. spectrum of $[NBu^n_4]_2[Ni(C_3Se_5)_2]$ at 1 430 $cm^{-1}$ is shifted to 1 380 $cm^{-1}$ upon the one-electron oxidation, which is similar to the low-frequency shift of ν(C=C) bands of $C_3S_5$-metal complexes upon oxidation.[36] However, the i.r. spectra of the further oxidized species, (**8**) and (**9**), were too broad to observe the bands.

The e.s.r. spectrum of (**7**) measured in acetonitrile at room temperature shows an isotropic signal at $g = 2.095$, which can be compared with that of $[NBu^n_4][Ni(C_3S_5)_2]$ ($g = 2.04$).[36] However, e.s.r. signals of the further oxidized species, (**8**) and (**9**), were too broad to be interpreted. This may be related to electron delocalization through the more effective conducting pathways of these complexes, which leads to much higher conductivities, as described later. Extreme broadening of signals was also observed for $[depz]_{0.35}[Ni(C_3S_5)_2]$ [depz = 1,4-diethylpyrazinium(2+)] which also shows a high electrical conductivity.[36]

*Electrical Conductivities.*—The complexes in this study behave as semiconductors in the temperature range measured (−30 to +30 °C). Electrical conductivities measured for compacted pellets at 25 °C are $1.2 \times 10^{-7}$ S $cm^{-1}$ (activation energy, $E_a = 0.37$ eV) for (**1**), $7.1 \times 10^{-7}$ S $cm^{-1}$ ($E_a = 0.25$ eV) for (**2**), and $6.9 \times 10^{-7}$ S $cm^{-1}$ ($E_a = 0.22$ eV) for (**3**). Conductivities of these complexes may arise from conduction pathways constructed with selenium–selenium contacts as described in the crystal structure of (**2**). These values can be compared with a conductivity of $7.1 \times 10^{-10}$ S $cm^{-1}$ for $[epy]_2[Cu(C_3S_5)_2]$ in which there is a one-dimensional chain arrangement through weak sulphur–sulphur contacts.[17] The $ttf^{\bullet+}$ radical cation complex (**4**) exhibits a somewhat higher conductivity [$1.4 \times 10^{-5}$ S $cm^{-1}$ ($E_a = 0.76$ eV)], which is possibly due to electrical conduction through a $ttf^{\bullet+}$ radical cation column.

Although the nickel complex (**5**) has a small conductivity ($5.0 \times 10^{-8}$ S $cm^{-1}$) for a compacted pellet at 25 °C, complex (**7**) exhibits a conductivity of $2.0 \times 10^{-4}$ S $cm^{-1}$ (measured for a single crystal along the *c* axis) at 25 °C. This arises from an electrical conduction pathway constructed with molecular interactions among the ligands through selenium–selenium contacts as shown in the crystal structure (Figures 4 and 5). The further oxidized complexes (**8**) and (**9**) exhibit higher conductivities of 0.21 ($E_a = 0.075$ eV) and 0.056 S $cm^{-1}$ ($E_a = 0.10$ eV), respectively, for compacted pellets at 25 °C. Thus, these complexes may have even more effective conduction pathways through the selenium–selenium interactions.

## Acknowledgements

We thank Professor K. Nakatsu, Kwansei Gakuin University, for use of the programs for the structure solution and refinement. This work was supported in part by a grant from Izumi Research and Technology Foundation.

## References

1 J. M. Williams, H. H. Wang, T. J. Emge, U. Geiser, M. A. Beno, P. C. W. Leung, K. D. Carlson, R. J. Thorn, and A. J. Schultz, *Prog. Inorg. Chem.*, 1987, **35**, 51.
2 M. Bosseau, L. Valade, L-P. Legros, P. Cassoux, M. Garbauskas, and L. V. Interrante, *J. Am. Chem. Soc.*, 1986, **108**, 1908 and refs. therein.
3 A. Kobayashi, H. Kim, Y. Sasaki, R. Kato, H. Kobayashi, S. Moriyama, Y. Nishino, K. Kajita, and Y. Sasaki, *Chem. Lett.*, 1987, 1819.
4 L. Brossard, H. Hundequint, R. Ribault, L. Valade, J-P. Legros, and P. Cassoux, *Synth. Met.*, 1988, **27**, B157.
5 R-M. Olk, W. Dietzsch, J. Mattusch, J. Stach, C. Nieke, E. Hoyer, and W. Meiler, *Z. Anorg. Allg. Chem.*, 1987, **544**, 199.
6 R-M. Olk, W. Dietzsch, R. Kirmse, J. Stach, and E. Hoyer, *Inorg. Chim. Acta*, 1987, **128**, 251.
7 R-M. Olk, A. Rohr, J. Sieler, K. Kohler, R. Kirmse, W. Dietzsch, E. Hower, and B. Olk, *Z. Anorg. Allg. Chem.*, 1989, **577**, 206.
8 G. Matsubayashi, K. Akiba, and T. Tanaka, *J. Chem. Soc., Dalton Trans.*, 1990, 115.
9 G. Matsubayashi and A. Yokozawa, *Chem. Lett.*, 1990, 355.
10 R-M. Olk, W. Dietzsch, and E. Hoyer, *Synth. React. Met.-Org. Chem.*, 1984, **14**, 915.
11 F. Wudl, *J. Am. Chem. Soc.*, 1975, **97**, 1962.

12 M. Main, S. E. Hull, L. Lessinger, G. Germain, J-P. Declercq, and M. M. Woolfson, 'A System of Computer Programs for the Automatic Solution of Crystal Structures from *X*-ray Diffraction Data, MULTAN 78,' University of York, 1978.
13 'International Tables for *X*-Ray Crystallography,' Kynoch Press, Birmingham, 1974, vol. 4.
14 C. K. Johnson, ORTEP II, Report ORNL 5138, Oak Ridge National Laboratory, Oak Ridge, Tennessee, 1976.
15 K. Ueyama, G. Matsubayashi, and T. Tanaka, *Inorg. Chim. Acta*, 1984, **87**, 143.
16 T. Nojo, G. Matsubayashi, and T. Tanaka, *Inorg. Chim. Acta*, 1989, **159**, 49.
17 G. Matsubayashi, K. Takahashi, and T. Tanaka, *J. Chem. Soc., Dalton Trans.*, 1988, 967.
18 O. Lindqvist, L. Andersen, J. Sieler, G. Steimecke, and E. Hoyer, *Acta Chem. Scand., Ser. A*, 1982, **36**, 855.
19 M. Bonamico and G. Dessey, *J. Chem. Soc. A*, 1971, 264.
20 L. Pauling, 'The Nature of the Chemical Bond,' 3rd edn., Cornell University, Ithaca, New York, 1960.
21 J. A. McCleverty, *Prog. Inorg. Chem.*, 1968, **10**, 49.
22 R. P. Burns and C. A. McAuliffe, *Adv. Inorg. Chem. Radiochem.*, 1979, **22**, 303.
23 D. J. Sandman, J. S. Stark, L. A. Acampora, L. A. Samuelson, G. W. Allen, S. Jansen, M. T. Jones, and B. M. Foxman, *Mol. Cryst. Liq. Cryst.*, 1982, **79**, 327.
24 W. B. Heuer, P. J. Squattrito, B. M. Hoffman, and J. A. Ibers, *J. Am. Chem. Soc.*, 1988, **110**, 792.
25 D. Snaathorst, H. M. Doesburg, J. A. A. J. Perenboom, and C. P. Keijzers, *Inorg. Chem.*, 1981, **20**, 2526.
26 D. J. Sandman, J. C. Stark, L. A. Acampona, L. A. Samuelman, G. W. Allen, S. Jansen, M. T. Jones, and B. M. Foxman, *Mol. Cryst. Liq. Cryst.*, 1984, **107**, 1.
27 W. B. Heuer, P. J. Squattrito, B. M. Hoffman, and J. A. Ibers, *J. Am. Chem. Soc.*, 1988, **110**, 792.
28 O. P. Andersen, C. M. Perkins, and K. K. Brito, *Inorg. Chem.*, 1983, **22**, 1267.
29 N. Aoi, G. Matsubayashi, and T. Tanaka, *J. Chem. Soc., Dalton Trans.*, 1987, 241.
30 J. L. Hughey, IV, T. G. Fawcett, S. M. Rudish, R. A. Lalancette, J. A. Potenza, and H. J. Schugar, *J. Am. Chem. Soc.*, 1979, **101**, 2617.
31 U. Sakaguchi and A. W. Addison, *J. Am. Chem. Soc.*, 1977, **99**, 5189.
32 R. Kirmse, R. Heber, and E. Hoyer, *Z. Chem.*, 1973, **13**, 385.
33 G. Matsubayashi, R. Shimizu, and T. Tanaka, *J. Chem. Soc., Dalton Trans.*, 1987, 1793.
34 G. Matsubayashi and A. Yokozawa, *J. Chem. Soc., Dalton Trans.*, in the press.
35 D. L. Coffen, J. Q. Chambers, D. R. Williams, P. E. Carrett, and N. D. Canfield, *J. Am. Chem. Soc.*, 1971, **93**, 2258.
36 Y. Sakamoto, G. Matsubayashi, and T. Tanaka, *Inorg. Chim. Acta*, 1986, **113**, 137.

*Received* 26*th April* 1990; *Paper* 0/01872D